Influence of time-periodic potentials on electronic transport in double-well structure

Li Chun-Lei(李春雷)† and Xu Yan(徐 燕)

College of Elementary Educational, Capital Normal University, Beijing 100048, *China*

(Received 12 September 2009; revised manuscript received 2 December 2009)

Within the framework of the Floquet theorem, we have investigated single-electron photon-assisted tunneling in a double-well system using the transfer matrix technique. The transmission probability displays satellite peaks on both sides of the main resonance peaks and these satellite peaks originate from emission or absorption photons. The single-electron resonance tunneling can be controlled through changing the applied harmonically potential positions, such as driven potential in wells, in barriers, or in whole double-well systems. This advantage should be useful in the optimization of the parameters of a transmission device.

Keywords: photon-assisted tunneling, transmission probability, quantum well
PACC: 7210, 7320D, 7335C

1. Introduction

Photon-assisted tunneling (PAT) that originates from harmonically driven mesoscopic systems has attracted more and more researchers' attention because of its potential applications in designing high-speed switching devices and high-frequency detectors, and so on. PAT implies that electrons with energy E can tunnel through a mesoscopic system via photon absorption and emission, then its energy $E\pm n\hbar\omega$ consists of a resonant condition. In order to research the transmission properties of electrons in time-periodic potentials, many methods have been developed. Experimentally, Dayem and Martin[1] carried out an experiment of quantum interaction between microwave and tunneling electrons in a sandwich structure and reported the multiphoton phenomenon. Kouwenhoven *et al.*[2] observed a quantised current in a lateral quantum dot with oscillating tunnel barriers. And they also experimentally observed the PAT through a GaAs/AlGaAs quantum dot with a microwave signal in 1994.[3] Oosterkamp *et al.*[4] studied interaction between microwave and electronic states in a quantum dot using PAT. Fujisawa and Tarucha[5] described PAT in quantum dot systems and reported the observed PAT current peak. By van der Wiel *et al.*[6] was investigated the influence of PAT in weakly- and strongly-coupled quantum dots. Very recently, single-particle transmission in strongly driven double-well potentials was reported by Kierig *et al.*[7] They studied influences of frequency and amplitude on single-particle transport.

While in the theoretical aspect, a number of researchers theoretically investigated electron PAT in the presence of harmonically driven potentials by using Green's function approach,[8−11] time-dependent perturbation theory,[12] multiple-scattering approach,[13] Floquet theory[14] combined with the transfer-matrix technique,[15−17] and so on. Wagner[18] studied transmission spectrum in a symmetric triple-barrier diode driven by a spatially uniform harmonic ac field. Li *et al.*[19,20] researched into electronic transport properties in quantum dot by using a recursion method. Sun *et al.*[21] investigated electron transport in double-coupled quantum dots driven by a microwave field. In these references, some researchers calculated PAT under the condition of oscillating quantum wells simultaneously with oscillating barriers. Others discussed PAT in double-barrier nanostructure where either the quantum well or the barriers were subjected to harmonically driven potential. So far, to our knowledge, almost no one has pointed out the differences between quantum well and quantum barrier subject to harmonic potential in double wells quantum structure.

Double-well system[22−26] have been intensively investigated for its technological applications in quantum information processing and low-dimensional semiconductor optoelectronic devices. It provides the basic necessity for exploring a two-qubit entangling gate caused by exchange interaction between the two

†Corresponding author. E-mail: lichunlei566@126.com
© 2010 Chinese Physical Society and IOP Publishing Ltd

electron states in the wells.

In this work, we present theoretical results for a single-electron PAT in a double-well system (DWS) with harmonically driven potential by using the transfer-matrix technique within the framework of Floquet theory. The transfer-matrix technique is an advantageous method in the theoretical investigation of transport properties[16,17,27,28] because any potential can be approximately divided into infinite stepwise constant potentials. The purpose of this work is to point out the different influences of driven quantum wells and driven quantum barriers on PAT in DWS. For simplicity, we limit the situation to a temperature $T = 0$ case where the electron–phonon interaction can be neglected. In Section 2, we give the solution of the time-dependent Schrödinger equation and construct the transfer-matrix for this system. In Section 3, we compare PAT in spatially uniformly driven DWS with oscillating quantum wells and oscillating quantum barriers. Finally, we give some conclusions in Section 4.

2. Model and method

In this paper, we consider a single-electron tunneling through a DWS. The single-electron Schrödinger equation can be written as

$$\mathrm{i}\,\hbar\frac{\partial}{\partial t}\Psi(z,t) = \mathrm{i}\,\hbar\frac{\hbar^2}{2\mu^*}\frac{\partial^2}{\partial z^2}\Psi(z,t) + V(z,t)\Psi(z,t), \quad (1)$$

where μ^* is the single-electron effective mass. $V(z,t)$ is the time-periodic potential (see Fig. 1). The potential with the oscillating barriers is given by

$$V(z,t) = \begin{cases} 0 & \text{(emitter and collector)}, \\ V_\mathrm{b} + V_1\cos(\omega t) & \text{(layers of barrier)}, \\ V_\mathrm{w} & \text{(layers of well)}, \end{cases} \quad (2)$$

or with the oscillating wells it is given by

$$V(z,t) = \begin{cases} 0 & \text{(emitter and collector)}, \\ V_\mathrm{b} & \text{(layers of barrier)}, \\ V_\mathrm{w} + V_1\cos(\omega t) & \text{(layers of well)}, \end{cases} \quad (3)$$

where V_b and V_w are the static barrier height and well depth, respectively. The $V_1\cos(\omega t)$ is the applied field with amplitude V_1 and frequency ω.

Using the Floquet theorem,[29] when an electron incident to a harmonically driven region, it will be scattered into Floquet sideband. Thus, in regions of emitter and collector, the wave function can be written as

$$\Psi^\mathrm{e}(z,t) = \sum_{n=-\infty}^{\infty}(\mathrm{e}^{\mathrm{i}\,k_0 z - \mathrm{i}\,E_0 t/\hbar} + r_n\mathrm{e}^{-\mathrm{i}\,k_{en} z - \mathrm{i}\,E_n t/\hbar}), \quad (4)$$

$$\Psi^\mathrm{c}(z,t) = \sum_{n=-\infty}^{\infty}(t_n\mathrm{e}^{-\mathrm{i}\,k_{cn} z - \mathrm{i}\,E_n t/\hbar}), \quad (5)$$

where r_n and t_n are the probability of the reflecting and transmission waves in the nth sideband, respectively. $E_n = E_0 + n\hbar\omega$, with E_0 being the incident electron energy. The wave vectors in regions of emitter and collector are $k_{en} = k_{cn} = \sqrt{2\mu^*(E_0 + n\hbar\omega)}/\hbar$, and $\hbar\omega$ is the energy of one photon.

Since harmonically driven potential exists in quantum wells or quantum barriers in the DWS, this leads to the following wave functions in the DWS for oscillating quantum wells or barriers, respectively:

$$\Psi(z,t) = \begin{cases} \sum\limits_{n=-\infty}^{\infty}(a_n\mathrm{e}^{\mathrm{i}\,q_n^\mathrm{b} z} + b_n\mathrm{e}^{-\mathrm{i}\,q_n^\mathrm{b} z})\mathrm{e}^{-\mathrm{i}\,E_n t/\hbar}, & \text{(barriers)}, \\ \sum\limits_{n,m=-\infty}^{\infty}(a_m\mathrm{e}^{\mathrm{i}\,q_m^\mathrm{w} z} + b_m\mathrm{e}^{-\mathrm{i}\,q_m^\mathrm{w} z})J_{n-m}\left(\dfrac{V_1}{\hbar\omega}\right)\mathrm{e}^{-\mathrm{i}\,E_n t/\hbar}, & \text{(oscillating wells)}, \end{cases} \quad (6)$$

$$\Psi(z,t) = \begin{cases} \sum\limits_{n,m=-\infty}^{\infty}(a_m\mathrm{e}^{\mathrm{i}\,q_m^\mathrm{b} z} + b_m\mathrm{e}^{-\mathrm{i}\,q_m^\mathrm{b} z})J_{n-m}\left(\dfrac{V_1}{\hbar\omega}\right)\mathrm{e}^{-\mathrm{i}\,E_n t/\hbar}, & \text{(oscillating barriers)}, \\ \sum\limits_{n=-\infty}^{\infty}(a_n\mathrm{e}^{\mathrm{i}\,q_n^\mathrm{w} z} + b_n\mathrm{e}^{-\mathrm{i}\,q_n^\mathrm{w} z})\mathrm{e}^{-\mathrm{i}\,E_n t/\hbar}, & \text{(wells)}, \end{cases} \quad (7)$$

where the wave vector in the region of barrier(well) is $q_m^{\mathrm{b/w}} = \sqrt{2\mu^*(E_0 + m\hbar\omega - V_{\mathrm{b/w}})}/\hbar$, with $a_{n/m}$ and $b_{n/m}$ being constant coefficients; and $J_{n-m}(V_1/\hbar\omega)$ is the $(n-m)$th-order Bessel function of the first kind, and n and m are sidebands (Floquet channels) indexes. At each interface, by using the transfer-matrix technique and satisfying conditions for the wave functions and their derivatives, one can write the relations between reflection and transmission amplitudes r_n and t_n in matrix form as

$$\begin{pmatrix} t_{-N} \\ . \\ t_N \\ 0 \\ . \\ 0 \end{pmatrix} = M(X_{j+1})M(X_j)\cdots M(X_1) \begin{pmatrix} 0 \\ 1 \\ 0 \\ r_{-N} \\ . \\ r_N \end{pmatrix}, \tag{8}$$

where $M(X_j) = [M^{\mathrm{R}}(X_j)]^{-1}M^{\mathrm{L}}(X_j)$, X_j denotes the position of the jth interface. R and L denote the regions of the right and left side of the X_j interface, respectively.

Considering the matrix equation (8), the total transmission probability can be obtained

$$T = \sum_{n=-N}^{N} T_n = \sum_{n=-N}^{N} |\frac{k_{cn}}{k_0}| \mid t_n \mid^2 . \tag{9}$$

In general, the minimum number of Floquet channels depends on the relation: $N > V_1/\hbar\omega$.[29]

3. Results and discussion

We have considered the numerical calculations for a DWS consisting of $Al_xGa_{1-x}As/GaAs$ material with static potential $V_{\mathrm{b}} = 0.248$ eV, $V_{\mathrm{w}} = 0$ eV, and the effective mass $\mu^* = 0.0944\mu$,[30] where μ is the free electron mass. Widths of barriers and wells from left to right are 5, 3, 2, 3, and 5 nm. The potential profiles to which this Floquet scattering is applied are shown in Fig. 1 (for clarity, V_1 is enlarged in Fig. 1).

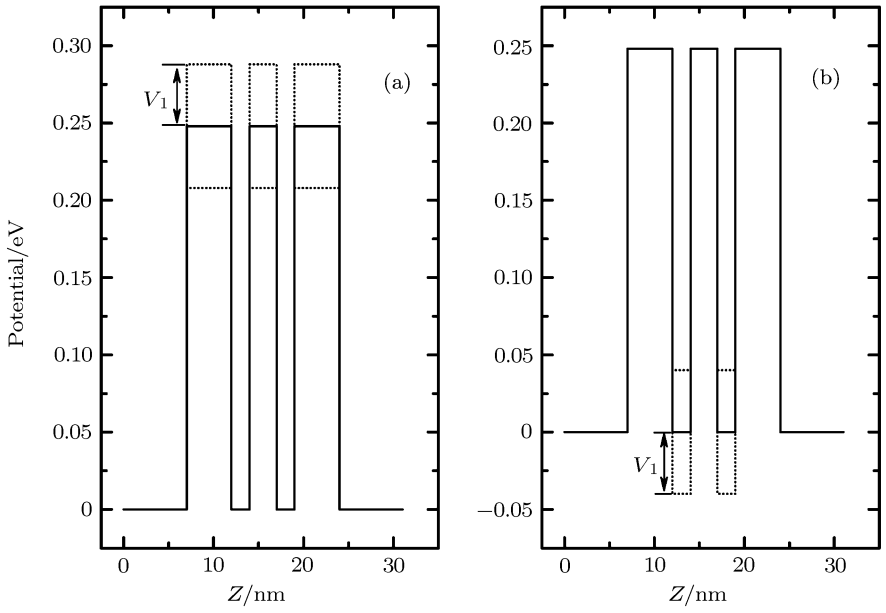


Fig. 1. Potential profile of a double-well structure. V_1 is the amplitude of the periodic potential. (a) oscillating quantum barriers, (b) oscillating quantum wells.

Figure 2 shows the total transmission probability as a function of the incident electron energy for different frequency of applied field ω. In Fig. 2, the applied field with amplitude $V_1 = 30$ meV, and the energy of photon $\hbar\omega$ changes from 10 to 50 meV. For clarity, each curve has been given an offset by 0.5 in Fig. 2. The top one shows transmission resonance without the PAT, that is, applied field $V_1 \cos(\omega t) = 0$, and there are two resonant split peaks positioned at $E_0^1 = 0.145$ eV and $E_0^2 = 0.186$ eV (indicated by vertical arrows in Fig. 2). This is due to the inter-wells coupling of the DWS. Considering the effect of PAT, some satellite peaks appear on both sides of the two main resonant peaks, and as the energy of photon increases, the satellite peaks move away from the two main resonant peaks. These satellite peaks appearing at positions $E_0^{1(2)} \pm n\hbar\omega$, where '+' and '−' denote the emission and absorption of n photons, respectively. In Fig. 2, the dotted and the solid-sloped lines indicate the positions of satellite peaks that belong to the same number of photon absorption and emission of E_0^1 and E_0^2.

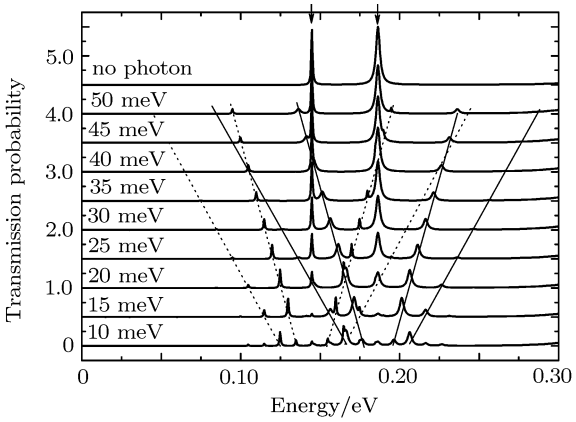


Fig. 2. The total transmission probability as a function of the incident electron energy for the energy of photon $\hbar\omega$ changed from 10 to 50 meV, and free-field(no photon).

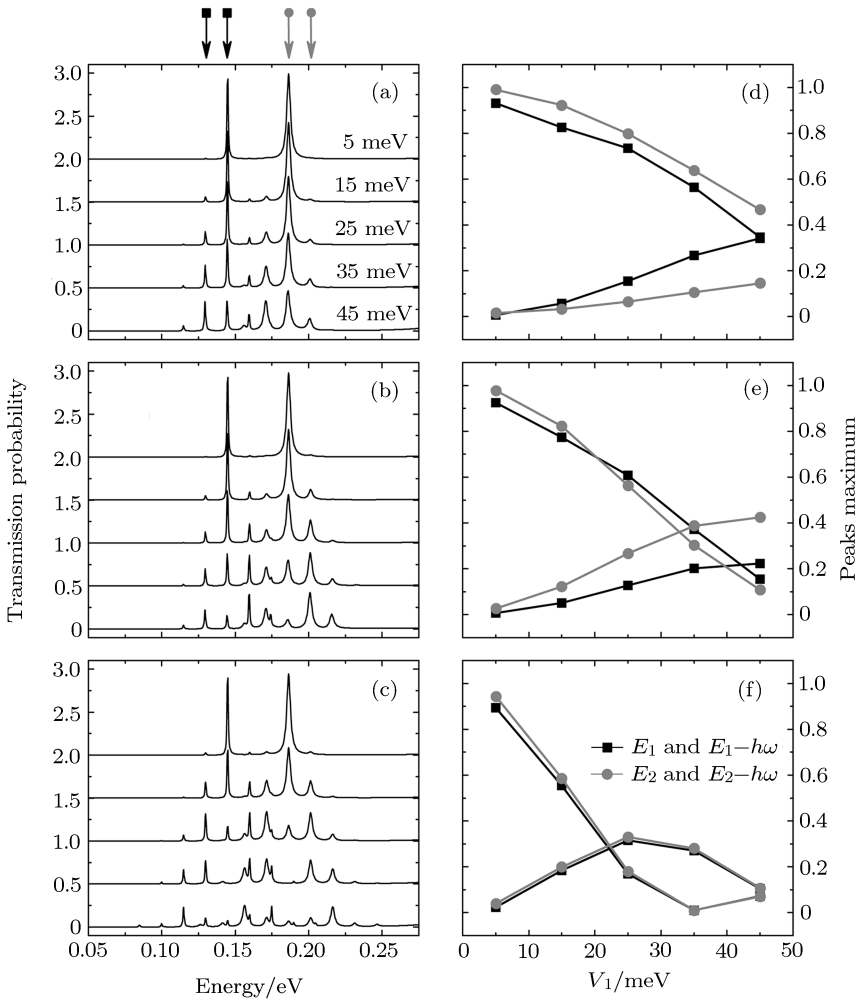


Fig. 3. (a), (b) and (c): The total transmission probability as a function of the incidence electron energy for different bias potentials (from 5 to 45 meV). (d), (e), and (f): Peaks maxima as functions of amplitude V_1 for oscillating barriers, oscillating wells, and whole oscillating DWS. The corresponding resonant peaks are indicated by vertical arrows with solid square and circle, respectively.

We now turn to considering the different effects of oscillating quantum barriers (Fig. 3(a)), oscillating quantum wells (Fig. 3(b)), and the whole oscillating DWS (Fig. 3(c)) on electron transport in the DWS. Figure 3 shows these results for the oscillation field with photon energy $\hbar\omega = 15$ meV and amplitudes $V_1 = 5$, 15, 25, 35, and 45 meV. For clarity, each curve has been given an offset by 0.5 in Figs. 3(a)–3(c). Figure 3 shows that, as the driven potential changes, the positions of the two main transmission peaks do not shift to lower or higher energy regions. This is due to the fact that the resonance-energy-level is dependent on structure parameters of DWS, especially quantum-well width. The satellite peaks' position, the same as in Fig. 2, depends on frequency of the driven potentials and has a relation of $E_0^{1(2)} \pm n\hbar\omega$.

As the amplitude of the harmonically driven potential increases, transmission probability displays drastic change as shown in Fig. 3. At low potential amplitude there is two main peaks with only some small satellite peaks. At high amplitude, however, the two main peaks lose its dominant intensity. For clarity, peaks maxima as functions of amplitude V_1 at different conditions (oscillating barriers, oscillating wells, and whole oscillating DWS) are plotted in Figs. 3(d), 3(e), and 3(f). The corresponding resonant peaks are indicated by vertical arrows with solid square and circle, respectively. The four resonant peaks are peaked at energies $E_0^1-\hbar\omega$, E_0^1, E_0^2, and $E_0^2+\hbar\omega$ (0.130, 0.145, 0.186, and 0.201 eV), respectively. Figure 3(d) shows that as the amplitude of driven barriers increases, the main transmission peaks (energies at E_0^1 and E_0^2) decrease and the satellite peaks increase. However, intensities of main peaks and satellite peaks are not reversed for $V_1 \leq 45$ meV. From Fig. 3(e), we observe that by increasing driven potential amplitude the peaks have more drastic change than in Fig. 3(d), and intensities of main peaks and satellite peaks are reversed for $V_1 \geq 35$ meV, due to the lifetime of quasi-bound levels at higher energy being shorter than those at lower energy region, so that electrons do not have enough time to interact with the driven barriers. However, in driven wells, electrons reflect back and forth several rounds, and consequently, transmission peaks show a very different shape in the driven wells. For the driven whole DWS, as shown in Figs. 3(f) and 3(c), the influence of driven potential on lower and higher resonant levels is almost in the same way, and intensities of main and satellite peaks are reversed for $V_1 \geq 22$ meV. When $V_1 \geq 25$ meV, as the amplitude of driven potential further increases, the peaks located at energy $E_0^{1(2)} \pm \hbar\omega$ decrease their intensities, however, the higher and lower resonant peaks ($E_0^{1(2)} \pm 2\hbar\omega$) increase.

4. Conclusion

Within the framework of the transfer matrix technique and the Floquet theorem, we have studied the influence of harmonically driven potential on single-electron transport in DWS for different situations, such as driven barriers, driven wells, and driven whole DWS. Numerical results demonstrated that frequency and amplitude of harmonic field strongly affected transmission probability; and driven wells, driven barriers, and driven whole DWS have quite different influences on electrons going into the different sidebands, arising from the emission and absorption of photons. These properties may be useful for the optimisation of the parameters of a transmission device, such as high-speed switching devices and high-frequency radiation sources and detectors.

References

[1] Dayem A H and Martin R J 1962 *Phys. Rev. Lett.* **8** 246

[2] Kouwenhoven L P, Johnson A T, van der Vaart N C, Harmans C J P M and Foxon C T 1991 *Phys. Rev. Lett.* **67** 1626

[3] Kouwenhoven L P, Jauhar S, Orenstein J, McEuen P L, Nagamune Y, Motohisa J and Sakaki H 1994 *Phys. Rev. Lett.* **73** 3443

[4] Oosterkamp T H, Kouwenhoven L P, Koolen A E A, VanderVaart N C and Harmans C J P M 1997 *Phys. Rev. Lett.* **78** 1536

[5] Fujisawa T and Tarucha S 1997 *Superlattices Microstruct.* **21** 247

[6] van der Wiel W G, de Franceschi S, Elzerman J M, Fujisawa T, Tarucha S and Kouwenhoven L P 2003 *Rev. Mod. Phys.* **75** 1

[7] Kierig E, Schnorrberger U, Schietinger A, Tomkovic J and Oberthaler M K 2008 *Phys. Rev. Lett.* **100** 190405

[8] Cai W, Zheng T F, Hu P, Lax M, Shum K and Alfano R R 1990 *Phys. Rev. Lett.* **65** 104

[9] Lefebvre R and Moiseyev N 2004 *Phys. Rev.* A **69** 062105

[10] Sun Q F, Wang J and Lin T H 1998 *Phys. Rev.* B **58** 13007

[11] Zhao H, Liao W H, and Zhao G H 2007 *Chin. Phys.* **16** 1748
[12] Iñarrea J, Platero G and Tejedor C 1994 *Phys. Rev.* B **50** 4581
[13] Burmeister G and Maschke K 1998 *Phys. Rev.* B **57** 13050
[14] Hagmann M J 1995 *Appl. Phys. Lett.* **66** 789
[15] Lu J D, Shao L, Hou Y L and Dai H M 2007 *Chin. Phys.* **16** 3080
[16] Wagner M 1995 *Phys. Rev.* A **51** 798
[17] del Valle C P, Lefebvre R and Atabek O 1999 *Phys. Rev.* A **59** 3701
[18] Wagner M 1998 *Phys. Rev.* B **57** 111899
[19] Li S S, Chang K and Xia J B 2003 *Phys. Rev.* B **68** 245306
[20] Li S S, Abliz A, Yang F H, Niu Z C, Feng S L and Xia J B 2003 *J. Appl. Phys.* **94** 5402
[21] Sun Q F, Wang J and Lin T H 2000 *Phys. Rev.* B **61** 12643
[22] Smyth J F, Awschalom D D, Samarth N, Luo H and Furdyna J K 1992 *Phys. Rev.* B **46** 4340
[23] Zhang C X, Nie Y H and Liang J Q 2008 *Chin. Phys.* B **17** 2670
[24] Aguado R and Platero G 1997 *Phys. Rev.* B **55** 12860
[25] Pu H, Zhang W and Meystre P 2002 *Phys. Rev. Lett.* **89** 090401
[26] Toropov A A, Sedova I V, Sorokin S V, Terent'ev Y V, Ivchenko E L and Ivanov S V 2005 *Phys. Rev.* B **71** 195312
[27] Leo J 1989 *Phys. Rev.* B **39** 5947
[28] Klymenko M V, Safonov I M, Shulika O V and Sukhoivanov I A 2008 *Phys. Stal. Sol.* (b) **245** 1589
[29] Li W and Reichl L E 1999 *Phys. Rev.* B **60** 15732
[30] Yong G, Li Y C, Kong X J and Wei C W 1994 *Phys. Rev.* B **50** 17249